MBY144	*cdc12-112 ura4-D18 leu1-32* h-	(Chang *et al.*, 1997)
MBY149	*sid2-250 ade6-21x ura4-D18 leu1-32* h-	(Balasubramanian *et al.*, 1998)
MBY1730	sec63-GFP *ura4-D18 leu1-32* h-	This study
MBY286 KGY702	*cdc16-116 leu1-32 ura4-D18 ade6-210* h+	(Minet *et al.*, 1979)
MBY671	ost1::GFP-ura4+ *ura4-D18 leu1-32* h-	This study
MBY758	*cdc15-140 ura4- leu1-32 ade6-210* h-	(Nurse *et al.*, 1976)
SO1364	sec13-GFP::ura4+ *ade6-216 leu1-32 ura4-D18* h+	This study
SO1509	sec24-GFP::ura4+ *ade6-216 ura4-D18 leu1-32* h+	This study
SO1511	anp1-GFP::ura4+ *ade6-216 ura4-D18 leu1-32* h+	This study
SO1517	sec72-GFP::ura4+ *ade6-216 ura4-D18 leu1-32* h+	This study
SO1626	sec24-GFP::ura4+ *ade6-216 leu1-32 ura4-D18 cdc16_116* h?	This study
SO1678	sec72-GFP::ura4+ *ade6-216 leu1-32 ura4-D18 cdc16_116* h?	This study
SO1696	anp1-GFP::ura4+ *ade6-216 leu1-32 ura4-D18 cdc16_116* h?	This study
SO2412	anp1- mCherry::ura4+ *ade6-216 leu1-32 ura4-D18* h+	This study
SO2423	sec24-GFP::ura4+ anp1-mCherry::ura4+ *ade6-21x leu1-32 ura4-D18* h?	This study
SO2427	uch2-mCherry::ura4+ *ade6-216 leu1-32 ura4-D18* h+	This study
SO2479	sec13-GFP::ura4+ rlc1-RFP::ura4+ *ade6-21x leu1-32 ura4-D18* h?	This study
SO2481	sec24-GFP::ura4+ rlc1-RFP::ura4+ *ade6-21x leu1-32 ura4-D18* h?	This study
SO2482	anp1-GFP::ura4+ rlc1-RFP::ura4+ *ade6-21x leu1-32 ura4-D18* h?	This study
SO2484	sec72-GFP::ura4+ rlc1-RFP::ura4+ *ade6-21x leu1-32 ura4-D18* h?	This study
SO2524	sec24-GFP::ura4+ rlc1-RFP::ura4+ *cdc15-140* pREP1-mad2 *ade6-21x leu1-32 ura4-D18* h?	This study

SO2525	anp1-GFP::ura4+ rlc1-RFP::ura4+ *cdc15-140* pREP1-mad2 *ade6-21x leu1-32 ura4-D18* h?	This study
SO2526	sec72-GFP::ura4+ rlc1-RFP::ura4+ *cdc15-140* pREP1-mad2 *ade6-21x leu1-32 ura4-D18* h?	This study
SO2527	sec24-GFP::ura4+ rlc1-RFP::ura4+ *cdc25-22* pREP1-cdc15 *ade6-21x leu1-32 ura4-D18* h?	This study
SO2800	sec24-GFP::ura4+ uch2-mCherry::ura4+ *ade6-21x leu1-32 ura4-D18* h?	This study
SO2801	anp1-GFP::ura4+ uch2-mCherry::ura4+ *ade6-21x leu1-32 ura4-D18* h?	This study
SO2802	sec72-GFP::ura4+ uch2-mCherry::ura4+ *ade6-21x leu1-32 ura4-D18* h?	This study
SO2803	sec24-GFP::ura4+ uch2-mCherry::ura4+ *cdc12-112 ade6-21x leu1-32 ura4-D18* h?	This study
SO2804	anp1-GFP::ura4+ uch2-mCherry::ura4+ *cdc12-112 ade6-21x leu1-32 ura4-D18* h?	This study
SO2805	sec72-GFP::ura4+ uch2-mCherry::ura4+ *cdc12-112 ade6-21x leu1-32 ura4-D18* h?	This study
SO2806	sec24-GFP::ura4+ uch2-mCherry::ura4+ *sid2-250 ade6-21x leu1-32 ura4-D18* h?	This study
SO2807	anp1-GFP::ura4+ uch2-mCherry::ura4+ *sid2-250 ade6-21x leu1-32 ura4-D18* h?	This study
SO2808	sec72-GFP::ura4+ uch2-mCherry::ura4+ *sid2-250 ade6-21x leu1-32 ura4-D18* h?	This study
SO2942	ost1-GFP::ura4+ rlc1-RFP::ura4+ *ura4-D18 leu1-32* h?	This study
SO2943	sec63-GFP::ura4+ rlc1-RFP::ura4+ *ura4-D18 leu1-32* h?	This study
SO2997	anp1-mCherry::ura4+ sec72-eGFP::ura4+ *ade6-21x leu1-32 ura4-D18* h?	This study
SO3023	ost1-mCherry *ade6-210 leu1-32 ura4-D18* h+	This study
SO3026	sec72-GFP::ura4+ anp1-mCherry::ura4+ *ade6-216 ura4-D18 leu1-32* h?	This study
SO3041	sec24-GFP::ura4+ uch2-mCherry::ura4+ *cdc4-8 ade6-21x leu? ura4-D18* h?	This study
SO3042	anp1-GFP::ura4+ uch2-mCherry::ura4+ *cdc4-8 ade6-21x leu? ura4-D18* h?	This study
SO3043	sec72-GFP::ura4+ uch2-mCherry::ura4+ *cdc4-8 ade6-21x leu? ura4-D18* h?	This study
SO3045	sec24-GFP ost1-mCherry::ura4+ *ade6-21x leu1-32 ura4-D18* h?	This study

SO3046	*cdc4-8 ade6-21x leu? ura4-D18* h-	(McCollum *et al.*, 1995)
SO3047	sec24-GFP::ura4+ rlc1-mCherry::ura4+ *ade6-M21x leu1-32 ura4-D18* h?	This study
SO3050	sec24-eGFP::ura4+ rlc1-mCherry::ura4+ *cdc15-140 ade6-M21x leu1-32 ura4-D18* h?	This study
SO3121	sec24-GFP::ura4+ *myo4* ::ura4+ *myo5* ::ura4+ *ade? leu? ura4-D18* h?	This study

Supplemental movie legends

Supplemental Movie 1. COPII coat protein Sec24p-GFP marks moderately stable tER sites in fission yeast.
Time-lapse sequence of cells expressing *cis*-Golgi marker Sec24p-GFP. Arrows indicate stable tER sites. Shown are the single-plane epifluorescence microscopy images taken every 5 seconds.

Supplemental Movie 2. Golgi biogenesis.
Time-lapse sequence of cells expressing *cis*-Golgi marker Anp1p-mCherry (red). Arrows indicate sites of cis-Golgi cisternae biogenesis. Time-lapse images were generated using spinning-disk confocal imaging system. Image stacks consisted of 10 sections of 0.5 μm spacing taken every ~6 seconds. Three-dimensional images of each stack were combined into a QuickTime movie using Volocity software package.

Supplemental Movie 3. Golgi maturation dynamics are consistent with the cisternal maturation model.
Time-lapse sequence of cells expressing COPII vesicle marker Sec24p-GFP (green) and *cis*-Golgi marker Anp1p-mCherry (red). Arrows indicate the site of a Golgi cisternae maturing. Time-lapse images were generated using spinning-disk confocal imaging system. Image stacks consisted of 9 sections of 0.5 μm spacing taken every ~6 seconds. Three-dimensional images of each stack were combined into a QuickTime movie using Volocity software package.

Supplemental figure legend

Supplemental Figure 1. Spatial distribution of the endoplasmic reticulum throughout the cell cycle.
(A) Endoplasmic reticulum localization marked by Ost1p-GFP (top row of images) in interphase (first column), mitosis (second column), early and late septation (third and fourth column). The cell cycle stage was deduced by the morphology of the actomyosin ring marker Rlc1p-mRFP (second row from the top) and the DIC image (not shown). Shown is the maximum projection image of the z-stack obtained by epifluorescence imaging. Epifluorescence images of 50 individual cells at the same stage of the cell cycle expressing Sec24p-GFP were standardized and compared to produce an averaged image (third row from the top, for details see Materials and Methods). The horizontal axis indicates position along the cell axis in percentages of cell length and the vertical axis indicates fluorescence intensity in arbitrary units.

(B) Shown is the maximum projection images of z-stacks obtained by epifluorescence microscopy of *S. pombe* cells expressing tER marker Sec24p-GFP (green, left panel) and ER marker Ost1p-mCherry (red, center panel). Polarization of the tER marker protein in dividing cells occurred independently of the ER accumulation (overlay, right panel).

Supplemental Figure 2. Accumulation of the early secretory pathway compartments at the site of division is statistically significant.
(A) Statistical significance of differences in fluorescence signal between two axial positions in cells expressing tER marker Sec24p-GFP during interphase (first column), mitosis (second column), early and late septation (third and fourth column). Epifluorescence maximum projection images of z-stacks of 50 individual cells at the same stage of the cell cycle (determined based on Rlc1p-RFP signal and DIC images) were standardized and compared to produce the p-values (for details see Materials and Methods).

(B) Statistical significance of differences in fluorescence signal between two axial positions in cells expressing *cis*-Golgi marker Anp1p-GFP, imaging and analysis as in (A).

(C) Statistical significance of differences in fluorescence signal between two axial positions in cells expressing *trans*-Golgi marker Sec72p-GFP, imaging and analysis as in (A).

Supplemental Figure 3. Actomyosin ring assembly is required for secretory pathway (SP) recruitment to the division site
(A) Temperature sensitive *cdc4-8* mutant cells expressing Sec24p-GFP (top row) and the nuclear marker Uch2p-mCherry (bottom row) were imaged upon entry into anaphase after previously being synchronized in G2 by elutriation, transferred into fresh medium and allowed to grow at 36ºC (left column) and 24ºC (right column). Shown is the maximum projection image of the z-stack obtained by epifluorescence imaging.

(B) Temperature sensitive *cdc4-8 mu*tant cells expressing Anp1p-GFP (top row) and the nuclear marker Uch2p-mCherry (bottom row) were treated as in (A).

(C) Temperature sensitive *cdc4-8* mutant cells expressing Sec72p-GFP (top row) and the nuclear marker Uch2p-mCherry (bottom row) were treated as in (A).

(D) Quantitation of Sec24p-GFP, Anp1p-GFP and Sec72p-GFP polarization under experimental conditions described in (A) (n=250 cells per sample).

Supplemental Figure 4. 10μM Latrunculin A causes complete depolymerization of the actin cytoskeleton in *S. pombe*.
Cells expressing Sec24p-GFP and Uch2p-mCherry were grown overnight at 24°C and treated for 30 minutes with either 10μM LatA dissolved in DMSO (left column) or DMSO alone (right column). Culture samples were taken and stained for actin (phalloidin, top row) and DNA (DAPI, bottom row) indicating that 30 minute treatment with 10μM LatA is sufficient for complete depolymerization of the actin cytoskeleton in *S. pombe*. Identical results were obtained for wild-type cells (data not shown).

Supplemental Figure 5. The Septation Initiation Network is required for maintenance but not for the initial recruitment of the early secretory pathway compartments at the division site.
(A) *sid2-250* cells expressing Sec24p-GFP (first and third row from the top) and Uch2p-mCherry (second and fourth row from the top) were grown overnight at 24ºC and imaged at either 24ºC (top two panels) or shifted to 36ºC (bottom two panels) for 1 hour prior to imaging.. Shown is the maximum projection image of the z-stack obtained by time-lapse spinning disk confocal imaging. Numbers correspond to time in minutes.

(B) *sid2-250* cells expressing Anp1p-GFP (first and third row from the top) and Uch2p-mCherry (second and fourth row from the top) were treated as in (A).

(C) *sid2-250* cells expressing Sec72p-GFP (first and third row from the top) and Uch2p-mCherry (second and fourth row from the top) were treated as in (A).

Supplemental Figure 6. Type V myosins are not required for tER polarization at the division site.
*myo4*Δ *myo5*Δ cells expressing Sec24p-GFP were grown overnight at 24°C and imaged using light (bottom, single plane image) and epifluorescence (top, maximum projection image of the z-stack) microscopy.

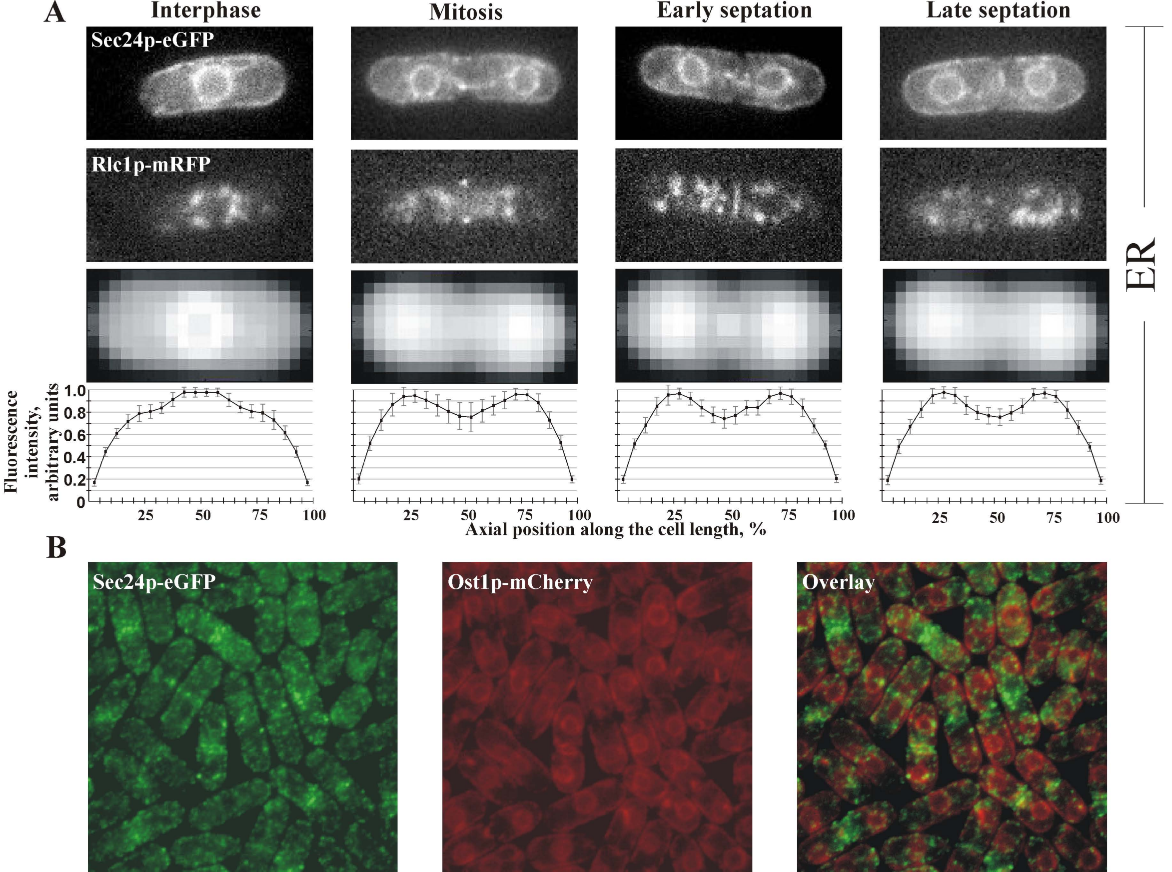
A
Interphase
Mitosis
Early septation
Late septation
Sec24p-eGFP
Rlc1p-mRFP
ER
Fluorescence intensity, arbitrary units
1.0
0.8
0.6
0.4
0.2
0
25
50
75
100
Axial position along the cell length, %
B
Sec24p-eGFP
Ost1p-mCherry
Overlay

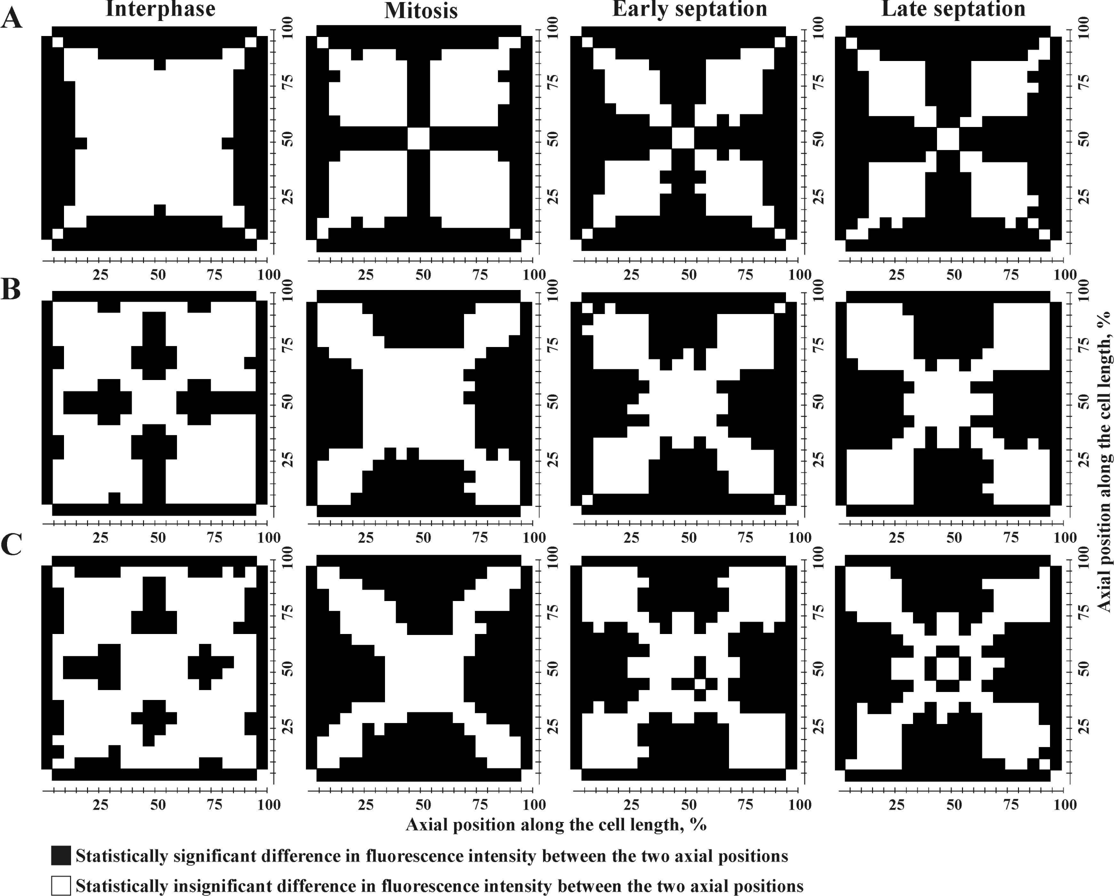
A
B
C
Interphase
Mitosis
Early septation
Late septation
25
50
75
100
Axial position along the cell length, %
Axial position along the cell length, %
Statistically significant difference in fluorescence intensity between the two axial positions
Statistically insignificant difference in fluorescence intensity between the two axial positions

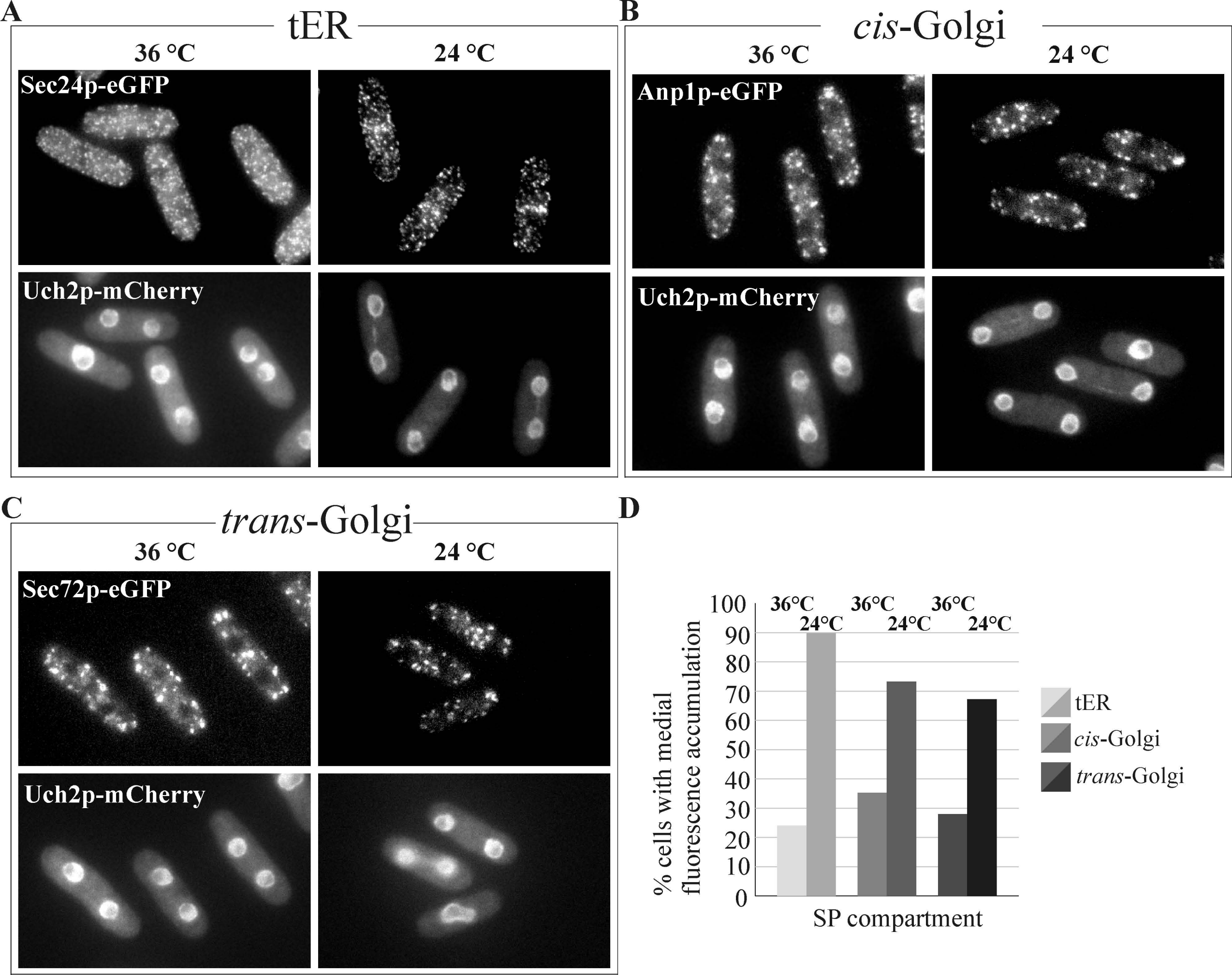

A
tER
36 °C
24 °C
Sec24p-eGFP
Uch2p-mCherry
B
cis-Golgi
36 °C
24 °C
Anp1p-eGFP
Uch2p-mCherry
C
trans-Golgi
36 °C
24 °C
Sec72p-eGFP
Uch2p-mCherry
D
% cells with medial fluorescence accumulation
100
90
80
70
60
50
40
30
20
10
0
36°C
24°C
36°C
24°C
36°C
24°C
SP compartment
tER
cis-Golgi
trans-Golgi

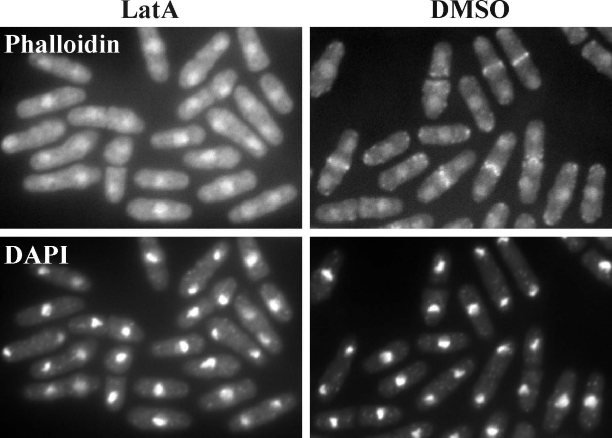
LatA
DMSO
Phalloidin
DAPI

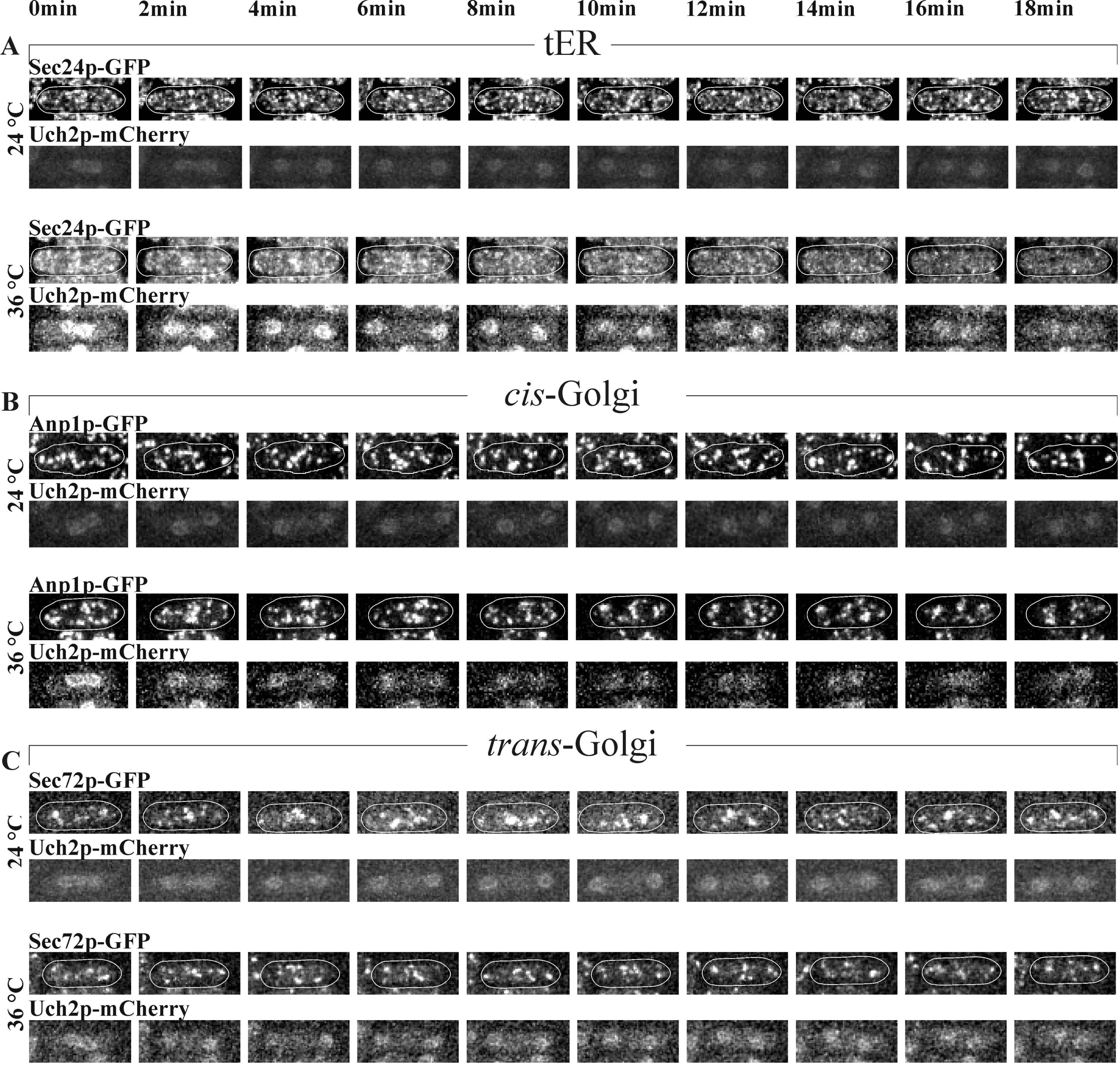
0min
2min
4min
6min
8min
10min
12min
14min
16min
18min
A
tER
Sec24p-GFP
24 °C
Uch2p-mCherry
Sec24p-GFP
36 °C
Uch2p-mCherry
B
cis-Golgi
Anp1p-GFP
24 °C
Uch2p-mCherry
Anp1p-GFP
36 °C
Uch2p-mCherry
C
trans-Golgi
Sec72p-GFP
24 °C
Uch2p-mCherry
Sec72p-GFP
36 °C
Uch2p-mCherry

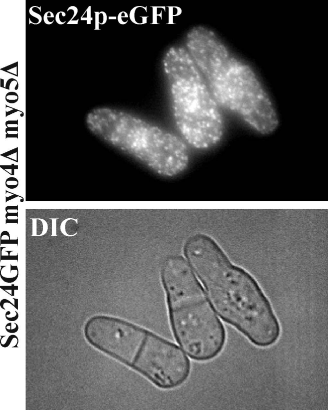
Sec24GFP myo4Δ myo5Δ
Sec24p-eGFP
DIC